Seismic Performance of RC Hollow Rectangular Bridge Piers Retrofitted by Concrete Jacketing Considering the Initial Load and Interface Slip

Made Suarjana[1,*], Daniel Dixon Octora[2] & Muhammad Riyansyah[1]

[1]Structural Engineering Research Group, Institut Teknologi Bandung,
Jalan Ganesha No. 10, Bandung 40132, Indonesia
[2]Directorate General of Highways, Ministry of Public Works and Housing Indonesia,
Jalan Pattimura No. 20, Jakarta 12110, Indonesia
*E-mail: msuarjana@itb.ac.id

Highlights:

- The effect of initial load and interface slip on the moment-curvature relationship of a retrofitted bridge pier was evaluated.
- The capacity of the retrofitted bridge pier was evaluated by considering both parameters with a monolithic approach.
- A plastic hinge model of the retrofitted bridge pier was made for pushover analysis.

Abstract. In design practice, the assumptions that are used in retrofitting concrete structural elements often ignore the initial load and the interface slip on the contact surfaces between the old and the new concrete. The concrete structural elements that are loaded by the existing gravity load cause initial strain on the existing cross-section before jacketing is applied, while the interface does not act in a fully composite manner. In this study, a seismic performance evaluation using pushover analysis was performed of a damaged reinforced concrete bridge pier retrofitted with concrete jacketing, where the plastic hinge of the retrofitted elements was modeled by considering both parameters. The results showed that concrete jacketing could increase the capacity of the bridge structure. It was also found from the numerical result that the performance level of the bridge considering the initial load compared to the monolithic approach gave the same result since the initial load did not significantly affect the cross-sectional ultimate capacity. The difference between the ultimate capacity values computed by the two models was less than 7%. It was also shown that the interface slip had a significant effect with a slip coefficient smaller than 0.5.

Keywords: *bridge pier; concrete jacketing; initial load; interface slip; moment-curvature; plastic hinge model; pushover analysis; retrofit; seismic performance.*

1 Introduction

At present, road transportation is the main mode of transportation in Indonesia compared to other available modes, i.e. 90% of all goods and more than 95% of

Received July 29th, 2019, 1st Revision October 30th, 2019, 2nd Revision January 27th, 2020, Accepted for publication May 22nd, 2020.

DOI: 10.5614/j.eng.technol.sci.2020.52.3.4

all passengers in Indonesia use road transportation [1]. Bridges as part of road networks play a very important role by connecting two points that are blocked by obstacles such as rivers, railroads, or highways. In the service life of a bridge, the piers as seismic-critical elements can suffer damage or decrease in strength caused by various factors, such as earthquakes, foundation shifts caused by soil movement, and material degradation over time. Also, during the service life of a bridge, new regulations (code) with stricter requirements may be enforced. Both damages and code changes may cause the structure to no longer meet the requirements and retrofitting is needed to be able to restore or increase its strength and ductility.

There have been several incidents of damage to bridges in Indonesia, one of which concerned the Cisomang Bridge. The Cisomang Bridge is located in Cisomang Village, Purwakarta Regency, West Java Province. The bridge is part of the Purbaleunyi toll road, which connects Bandung and Jakarta, and is located at KM. 100+700. During around fifteen years of operation, the bridge has experienced a large foundation shift due to movements of the supporting clay shale soils. The accumulation of relatively slow movement of the clay shale soils caused deformations in several piers, with the largest deformation occurring in pier P2, measuring around 52.50 centimeters.

Different techniques were considered to retrofit the damaged bridge pier element. The technique that was chosen was concrete jacketing. Jacketing of reinforced concrete (RC) sections is a technique widely adopted in current engineering practice to retrofit damaged/weak members and to increase their strength and ductility. The method consists of casting a new RC layer (jacket) around the existing section and reinforcing it with additional longitudinal and transverse reinforcements to increase the cross-sectional capacity and the confinement effect of the member [2]. Seismic retrofitting of an existing bridge is generally more difficult than the design of a new bridge because of the various restrictions in the retrofit. This is because the main structural elements cannot be changed or replaced in seismic retrofitting, which narrows down the design and construction options [3].

Generally, two important things need to be considered in the application of concrete jacketing. Firstly, bridges often need to be retrofitted within a short time period without suspension of traffic, during which the retrofitting is applied to loaded structural elements under existing gravity load, causing initial strain to exist in it. Secondly, due to the nature of the jacketing, which results in two concrete layers being cast at different times, the occurrence of interface slip between the interconnected elements should be checked and considered in the section capacity of the cross-section.

Various researches have been carried out in the last twenty-five years to study the effect of initial load and interface slip on RC sections retrofitted with concrete jacketing. Ersoy, *et al*. [4] experimented with two series of jacketed columns under uniaxial and combined axial load and bending. The authors found that applying a strengthening jacket while the column was loaded functioned similarly under uniaxial loading compared to applying strengthening to columns that were unloaded. However, if the column is damaged to a level requiring repair, unloading may have more influence on the capacity of the column under uniaxial loading. Repaired columns under combined loading attain less rigidity than monolithic columns, while strengthened columns reach similar levels as monolithic columns. Strength is not influenced significantly by monotonic or cyclic loading history.

Julio, *et al.* [5], Julio and Branco [6], and Vandoros and Dritsos [7] found that the initial load has a negligible impact on the capacity of a section retrofitted with concrete jacketing and the effect of slip between the old-new concrete interface plays a lesser role. If the old concrete surface is not roughened, the reduction of composite phenomena, in terms of the flexural capacity, is almost 10% [2]. In a more recent analytical study on beams, by Alhadid and Youssef [8], it was found that initially loaded beams experience more ductility when the additional jacket steel bars are unstressed at the moment the partial interaction between the core and the jacket commences. The influence of slip on reducing the flexural stiffness of the jacketed beams becomes less pronounced when jacketing takes place at higher initial load.

The present study evaluated the effect of initial load and interface slip by non-linear section analysis of an RC section retrofitted with concrete jacketing and investigated the seismic performance of the bridge.

2 Bridge Description

To evaluate the effect of concrete jacketing on the seismic performance of bridge structures, a case study was conducted on an existing bridge in a toll road in Indonesia that has suffered serious damage in a pier element to which retrofitting has already been applied by concrete jacketing. The bridge pier element was cracked because of foundation shift due to the accumulation of soil movement caused by an active river.

The bridge has a total length of 252.127 meters, with a seven-span configuration supported by two abutments (A1 and A2) and six piers (P0, P1, P2, P3, P4, and P5), where P2 and P3 have the same height of 42.810 meters, and the highest pier, P4, is 46.451 meters high. The superstructure of the bridge consists of PCI beams

with a simple span (A1-P0, P0-P1, P4-P5, and P5-A2) and a continuous-integral span (P1-P2-P3-P4), as shown in Figure 1.

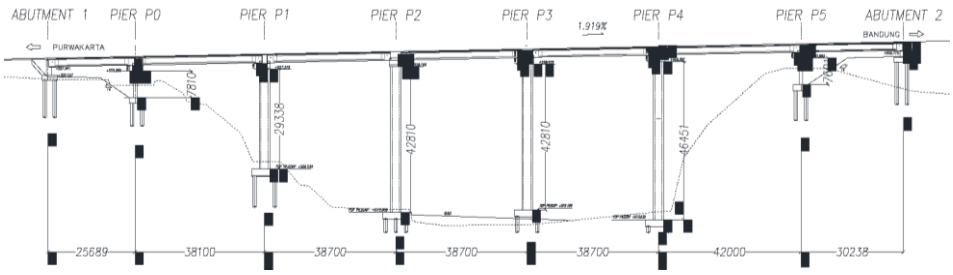

Figure 1 The geometry of the bridge model: long section of the bridge.

The bridge structure was completed in 2005 with seismic load demand according to the old Indonesian seismic design code [9]. The existing bridge piers have two different cross-section geometries, i.e. a solid rectangle for P0 and P5 and a rectangular hollow for P1-P4. The details of the cross-section geometries and the steel reinforcements of the bridge pier elements are tabulated in Table 1.

Table 1 Details of geometry and reinforcement of bridge piers.

Bridge Pier	Type	Section geometry			Longitudinal Bars	Transverse bars	
		Width (mm)	Height (mm)	Thickness (mm)		End-region	Mid-region
P0	Solid	1000	1250	-	34 D32	D13-100	D13-250
P1	Hollow	3100	3600	400	140 D22	D16-100	D13-150
P2	Hollow	3100	3600	400	112 D22	D16-100	D13-250
P3	Hollow	3100	3600	400	112 D22	D16-100	D13-250
P4	Hollow	3100	3600	400	100 D22	D16-100	D13-250
P5	Solid	1000	1250	-	36 D32	D13-100	D13-250

Based on the results of field investigations conducted by LAPI ITB in 2016 [10] it was found that several bridge piers had been displaced and damage was caused to piers P0, P1, P2, and P5. The largest displacement occurred in pier P2, measuring around 52.50 cm. Table 2 shows the displacement of the bridge piers.

Several retrofitting techniques have been applied to retrofit the damaged bridge piers, namely short-term (temporary) and long-term (permanent) retrofitting. To avoid further damage temporary retrofitting was carried out, such as grouting in the cracks of the RC sections, FRP jacketing, and steel foundation strutting to stop further movement of the base of the bridge piers. Furthermore, permanent retrofitting by RC jacketing was applied to restore and increase the capacity of the damaged elements and to withstand the external load on the bridge structure during the service life of the bridge.

The material properties used in RC jacketing were chosen to be the same as the existing material. An illustration of the cross-section geometry of the retrofitted pier P2 is shown in Figure 2 and a summary of the RC jacketing applied to the damaged bridge piers is tabulated in Table 3.

Table 2 Displacement data of bridge piers.

Bridge pier	Longitudinal		Transversal	
	Relative displacement (m)	Direction	Relative displacement (m)	Direction
P0A	0.134	Purwakarta	0.103	B
P0B	0.153	Purwakarta	0.073	B
P0C	0.118	Purwakarta	0.040	A
P0D	0.071	Purwakarta	0.089	A
P1A	0.264	Purwakarta	0.124	A
P1B	0.244	Purwakarta	0.264	A
P2A	0.525	Purwakarta	0.274	A
P2B	0.419	Purwakarta	0.143	A
P3A	0.055	Bandung	0.056	B
P3B	0.095	Purwakarta	0.057	B
P4A	0.119	Bandung	0.033	A
P4B	0.120	Bandung	0.069	A
P5A	0.005	Purwakarta	0.075	Bandung
P5B	0.003	Bandung	0.062	Bandung
P5C	0.003	Bandung	0.035	Bandung
P5D	0.001	Bandung	0.073	Bandung

Note: A, B, C, and D indicate the number of columns of each bridge pier.

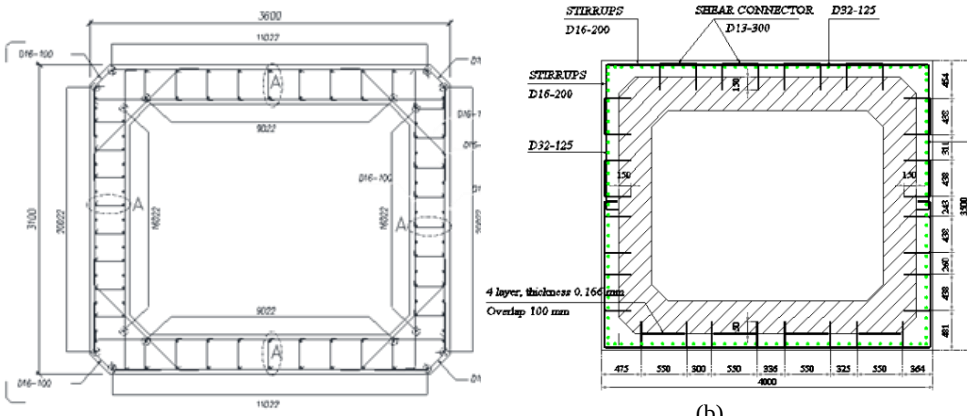

(a) (b)

Figure 2 Cross-section geometry: (a) existing, (b) retrofitted.

Table 3 RC jacketing application to damaged bridge piers.

Bridge pier	Pier type	Retrofit Type	Details of retrofitting			
			Thickness (mm)	Long. steel	Trans. steel	Shear connector
P0	Solid	RC jacketing	250	65 D25	D13-200	D13-300
P1	Hollow	RC jacketing	200	120 D22	D16-200	D13-300
P2-Bottom	Hollow	RC jacketing	200	120 D22	D16-200	D13-300
P2-Top	Hollow	Steel jacketing	20	-	-	-
P5	Solid	RC jacketing	250	62 D25	D13-200	D13-300

3 Non-Linear Section Analysis of RC Section with Jacketing

The main purpose of the non-linear section analysis is to obtain the moment-curvature (M-φ) relationship through a fiber section approach. The section is divided into three regions (cover, core, and steel), where all of them are discretized into a finite number of segments and each segment has an orientation towards a neutral axis. The initial load and interface slip in the non-linear analysis of the RC sections retrofitted with concrete jacketing was calculated in the section analysis by considering the discontinuous strain, as illustrated in Figure 3.

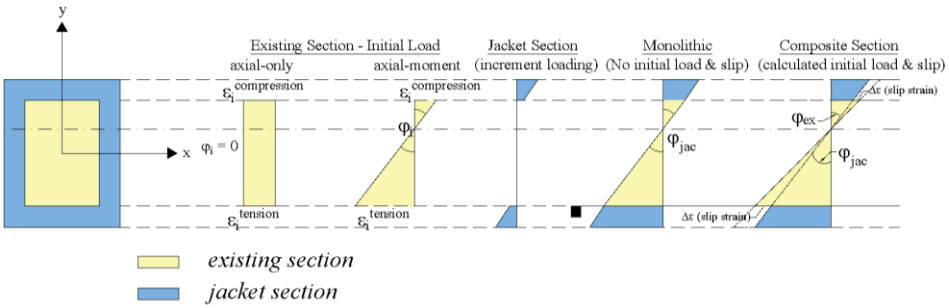

Figure 3 Strain profile of retrofitted section with RC jacketing considering the initial load and interface slip.

Theoretically, the relationship of moment-curvature at the level of load can be obtained by increasing the concrete strain, ε_{cm}, in the extreme compression fiber or by increasing the curvature, φ [11]. For each value of ε_{cm} or φ, there will be a neutral axis (zero strain position) that meets the force equilibrium requirements.

3.1 Proposed Calculation Algorithm and Assumptions

Basically, the calculation algorithms for the RC sections with and without jacketing for determining the moment-curvature relationship are the same. The fundamental difference is the constitutive model for confined concrete with

jacketing, where the total effective lateral pressure of the core is generated by both the existing and the jacketing stirrups/hoops [12]. Moreover, by taking into account the initial load due to the existing gravity load and the interface slip between two concrete elements cast at different times, the stress calculation for each segment in the RC section with jacketing can be calculated by modifying the strain [12]. Furthermore, it is assumed that the flexural stiffness of the damaged and the existing sections is the same due to the temporary repairs applied before jacketing.

3.1.1 Confinement Effectiveness Coefficient for RC Section with Jacketing

The method conducted by Ong, *et al.* [13] was adopted, which is based on the model proposed by Mander, *et al.* [14]. The effectively confined area of the core, the existing cover, and the jacket also have to be calculated. For the core, the effective lateral confining stress arising from the existing and jacketing confinement, $f_{l,core}^{'}$, can be calculated as follows:

$$f_{l,core}^{'} = \frac{1}{2} k_{e,ex} \rho_{s,ex} f_{yh,ex} + \frac{1}{2} k_{e,jac} \rho_{s,jac} f_{yh,jac} \quad (1)$$

where, $\rho_{s,ex}$ and $\rho_{s,jac}$ are the volumetric ratio of the existing and the jacketing transverse confining steel, respectively; $k_{e,ex}$ and $k_{e,jac}$ are the confinement effectiveness coefficient arising from the existing and the jacketing confinement, respectively; $f_{yh,ex}$ and $f_{yh,jac}$ are the yield strength of the existing and the jacketing transverse confining steel, respectively.

For RC section with jacketing of a rectangular section, the area of the concrete core that is ineffectively confined is represented by the area of the parabolas that occur horizontally between ties of the longitudinal bars and vertically between the layers of the transverse hoop bars (Figure 4). The effectively confined concrete core area at the stirrup/hoop level (plan) can be obtained by subtracting the area of the parabolas containing ineffectively confined concrete. Figure 4(a) shows the two possible conditions of the parabolic arrangement at the stirrup/hoop level (plan), which is expressed as follows:

1. The first condition happens when the position of the parabolas is far outside of the concrete core. The confining effect will be maximum and the ratio between the confined core area and the core may be taken as unity, i.e.

$$\lambda = 1 \quad (2)$$

2. The second condition happens when the parabolas intersect the core. The ratio λ is given by:

$$\lambda = \frac{A_{cc,jac} - \sum_{i=1}^{n} \frac{2w'_{i,jac}m}{3}}{A_{cc,jac}} \tag{3}$$

where, $w'_{i,jac}$ is the base length of the parabola, m is the rise of the parabola inside the core, taken as $\frac{1}{4}w'_{i,jac}$, and $A_{cc,jac}$ is the area of the core minus the area of the longitudinal steel jacket.

Similarly, two possible conditions of the parabolic arrangement vertically between the layers of the transverse hoop bars (elevation) are also assumed to occur, as shown in Figure 4(b), which are expressed as follows:

1. The first condition occurs when the vertical parabola falls outside of the core. The effectively confined core area can be formulated by:

$$A_e = \lambda b_c d_c \tag{4}$$

2. The second condition occurs when the parabolas cross the core. The effectively confined core area can be formulated by:

$$A_e = \lambda \left[1 - \left(\frac{s'_j}{2b_c} - 2m\right)\right]\left[1 - \left(\frac{s'_j}{2d_c} - 2m\right)\right] \tag{5}$$

where, b_c and d_c are the concrete core dimension to centerline perimeter hoop in the x-direction and y-direction, respectively; s'_j is the clear vertical spacing between the jacket stirrups or hoop bars.

Based on the formulation that was derived above from Eqs. (2)-(5), the confinement effectiveness coefficient arising from jacketing confinement is formulated as follows:

$$k_{e,jac} = \frac{A_e}{A_{cc}} = \frac{\lambda \left[1 - \left(\frac{s'_j}{2b_c} - 2m\right)\right]\left[1 - \left(\frac{s'_j}{2d_c} - 2m\right)\right]}{A_c(1 - \rho_{cc,j}} \tag{6}$$

Eq. (6) is formulated for the second condition. If the first condition occurs, then the value of $k_{e,jac}$ will be maximum or taken as unity.

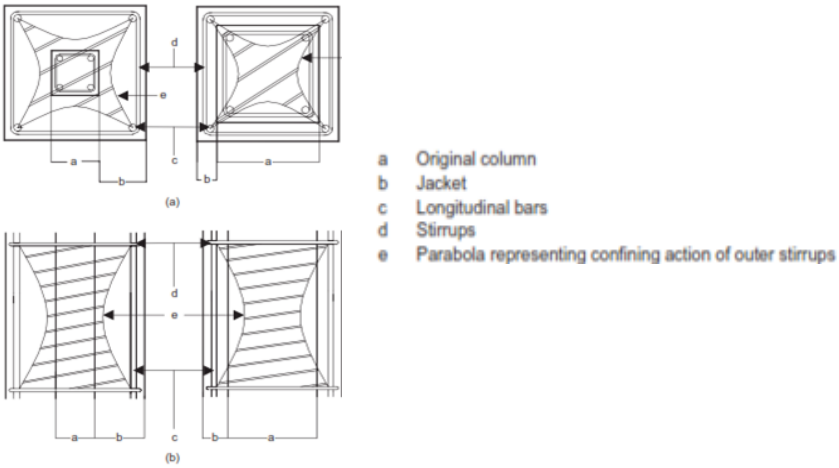

Figure 4 Effectively confined core with respect to the jacket stirrups/hoop: (a) at the level of the stirrups/hoop (plan), (b) between two adjacent levels of the stirrup/hoop (elevation) [13].

The ultimate compressive strain on the confined concrete of the RC section with jacketing follows the equation from Priestley, *et al.* [15], taking into account both the effects of the existing and the jacketing confinement, which can be calculated with the following formulations:

$$\varepsilon_{cu} = 0.004 + \frac{1.4\rho_{s,ex} f_{yh,ex} \varepsilon_{su,ex}}{f_{cc,ex}} + \frac{1.4\rho_{s,jac} f_{yh,\mathrm{jac}} \varepsilon_{su,\mathrm{jac}}}{f_{cc,\mathrm{jac}}} \tag{7}$$

where, $\rho_{s,ex}$ and $\rho_{s,jac}$ are the volumetric ratio of the existing and the jacketing transverse confining steel, respectively; $f_{yh,ex}$ and $f_{yh,\mathrm{jac}}$ are the yield strength of the existing and the jacketing transverse confining steel, respectively; $\varepsilon_{su,ex}$ and $\varepsilon_{su,\mathrm{jac}}$ is the steel strain at maximum tensile stress of the existing and the jacketing transverse confining steel; $f_{cc,ex}$ and $f_{cc,\mathrm{jac}}$ are the compressive strength of the confined concrete generated by the existing and the jacketing transverse confining steel, respectively.

3.1.2 Initial Load

The initial load in the M-φ calculation algorithm of the RC section with jacketing was calculated by modifying the strain value in the existing section, where the strain value in the existing section for each Δφ should be added with the initial strain of the existing section, whereas for the jacket section, the strain value for

each $\Delta\varphi$ is added with zero (no initial strain in the jacket section). The mathematical formulations for this explanation are formulated as follows:

For the existing section,

$$\varepsilon_{segment,ex[i]} = \left\{\left(y_c - y_{segment}[i]\right) \times \varphi[i]\right\} + \varepsilon_{initial} \tag{8}$$

For the jacket section,

$$\varepsilon_{segment,jac[i]} = \left\{\left(y_c - y_{segment}[i]\right) \times \varphi[i]\right\} + 0 \tag{9}$$

where, $\varepsilon_{segment,ex}$ and $\varepsilon_{segment,jac}$ are the strain at the existing and the jacket section, respectively; y_c is the neutral axis position from the top fiber of the section; $y_{segment}$ is the moment's arm of the segment, and $\varepsilon_{initial}$ is the initial strain of the existing section before the jacket was applied.

3.1.3 Interface Slip

When a concrete element is repaired by placing new concrete, full transfer of the interface shear forces must be provided at the contact surfaces of the interconnected elements, whereby the possibility of interface slip exists [16]. The mechanism for interface shear force transfer is known as shear friction. Figure 5 illustrates the condition of the interface slip. Its formulation, adopted from ACI 318M-14 (Sections 16.4.4 and 22.9), is as follows:

$$\phi V_{nh} \geq V_u \tag{10}$$

where, V_{nh} is the nominal interface shear strength, calculated according to ACI 318M-14, Table 16.4.4.2; V_u is the shear force corresponding to the plasticity of the top and base pier sections, and ϕ is the strength reduction factor.

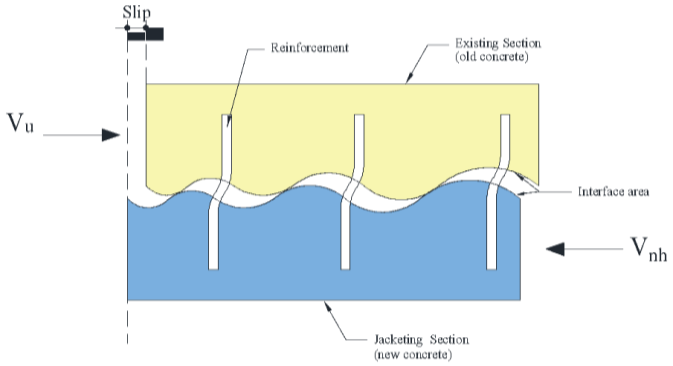

Figure 5 Shear friction and interface slip model.

To quantify the occurrence of slippage in the calculation for the RC section with jacketing, a simple method to estimate the reduction of the section's capacity is by multiplying the strain of each segment in the jacket section in Eq. (9) with the slip coefficient.

The slip coefficient is equal along the contact area with a variety of values > 0-1, where a value close to zero describes the bond at the interface being very minimal, while a value of one describes a perfect bond or full composite. The mathematical formulation for this is obtained by modifying Eq. (9) as follows:

$$\varepsilon_{segment,\,jac[i]} = \left\{\left(\left(y_c - y_{segment}\left[i\right]\right)\times\varphi\left[i\right]\right) + 0\right\}\times \text{slip coefficient} \tag{11}$$

The requirements for the minimum area of shear transfer reinforcement are based on ACI 318M-14, Section 16.4.6.1, i.e. $A_{v,\min}$ must be the greater of Eq. (12a) and (12b):

$$0.062\sqrt{f_c^{'}}\,\frac{b_w s}{f_y} \tag{12a}$$

$$0.35\,\frac{b_w s}{f_y} \tag{12b}$$

where b_w is the width of the cross section, s is the center-to-center spacing of the shear transfer reinforcement, $f_c^{'}$ and f_y are the concrete compressive strength and the yield strength of reinforcing steel, respectively.

3.2 Numerical Example

To demonstrate the proposed calculation algorithm that was derived above, this section examines the damaged pier P2 element that has already been retrofitted by concrete jacketing as an example. The initial load, represented by the initial curvature, is assumed to be below or above the yield curvature of the existing section (without jacketing), respectively, while the interface slip is applied to the jacket section with a coefficient of 0.05, 0.1, 0.5, 0.7, and 0.9, which works linearly in the slip plane along the contact area. Figure 2 and Table 4 show the cross-section geometry and material properties of the pier.

The capacity of the concrete components to resist all seismic demands except shear was assessed based on the expected material strength of unconfined and confined concrete as well as the reinforcing steel to provide a more realistic estimate of the earthquake load capacity [15,17,18].

Table 4 Parameters of cross-sectional geometry and material properties.

Parameter	Description	Dimension	Unit
B	Existing section width	3100	mm
H	Existing section height	3600	mm
$t_{c,ex}$	Existing concrete cover	50	mm
$t_{c,j}$	Jacketing concrete cover	50	mm
t_w	Hollow thickness	400	mm
t_j	Jacket thickness	200	mm
$D_{b,ex}$	Diameter existing of longitudinal bars	22	mm
$D_{b,j}$	Diameter jacketing of longitudinal bars	32	mm
$d_{t,ex}$	Diameter of existing stirrups/hoop	16	mm
s	Vertical spacing of existing stirrups/hoop bars	100	mm
$d_{t,j}$	Diameter of jacketing stirrups/hoop	16	mm
s_j	Vertical spacing of jacketing stirrups/hoop bars	200	mm
f_c'	Concrete compressive strength	30	MPa
f_{ce}'	Expected concrete compressive strength	$1.3 \times f_c'$	MPa
f_y	Yield strength of reinforcing steel	420	MPa
f_{ye}	Expected yield strength	$1.1 \times f_y$	MPa
E_c	Modulus of Elasticity of concrete	$4700\sqrt{f_c'}$	MPa
E_s	Modulus of Elasticity of reinforcing steel	200000	MPa

3.2.1 Section Discretization

The concrete section retrofitted with jacketing is discretized in four parts, i.e. the core, the existing outer cover, the inner jacket, and the cover (existing inner cover and jacket cover), as shown in Figure 6. The core, existing outer cover, and inner jacket are defined as confined material, while the existing inner cover and jacket cover are defined as unconfined material. Figure 6 illustrates the effectively confined core area of the section.

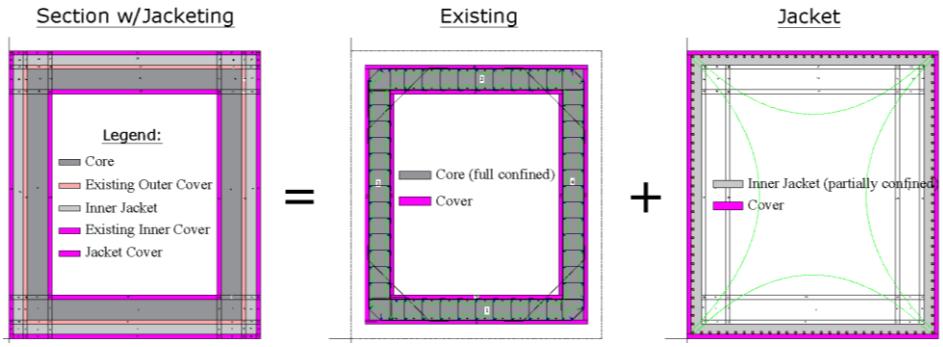

Figure 6 Section discretization and effectively confined core of the section.

The discretized concrete sections with jacketing are defined as follows:

1. Core : confined by existing and jacket confinement/stirrups

3. Existing outer cover: confined by jacket confinement/stirrups
4. Inner jacket : confined by jacket confinement/stirrups
5. Existing inner cover: unconfined material
6. Jacket cover : unconfined material

3.2.2 Stress-Strain of RC Section with Jacketing

As can be seen from Figure 7, there is an increase in the stress and strain of the core with jacketing reinforcement compared to the existing cross-section, which is due to the additional lateral stress contributed by the jacket stirrups.

The stress does not increase significantly because the ineffective area of the core is quite large due to the absence of ties on the jacket transverse reinforcement.

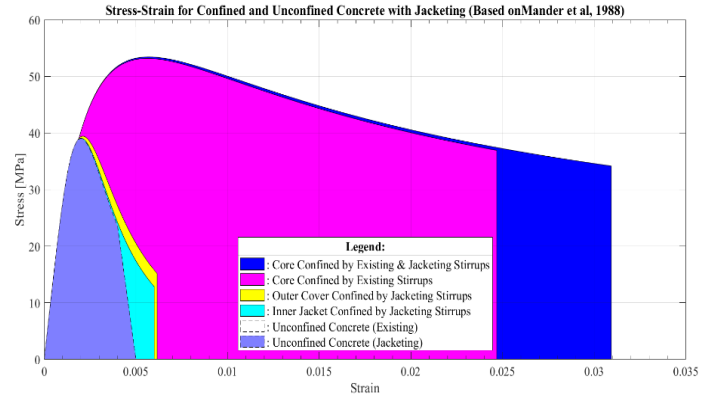

(a)

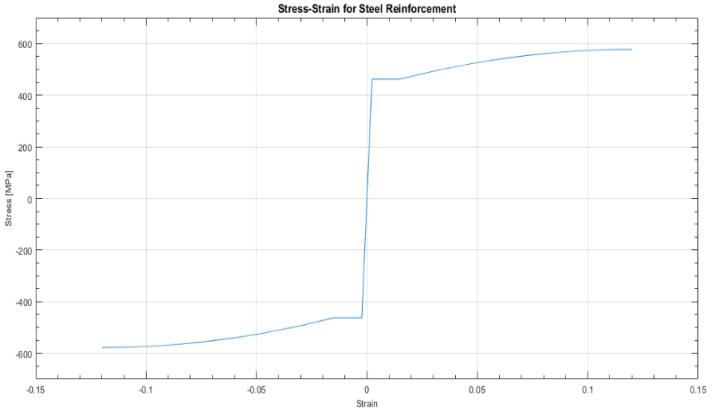

(b)

Figure 7 Stress-strain relationship of materials: (a) concrete, (b) steel bar.

3.2.3 Initial Load Effect

This section discusses the effect of the initial load on the M-φ relationship of the RC section with jacketing. Also, the comparison of the M-φ relationship of the RC section with jacketing, considering the initial load with a monolithic approach, is discussed by reviewing several cases, as described in Table 5. Figure 8 shows the comparison results for both scenarios, carried out in the strong-axis direction of the cross-section. Clearly, the jacketing strengthening could improve the capacity of the section by almost two times. For $M_i \le M_{y(pre-jacket)}$, the yield point after the jacket was applied is determined by the yield of the existing longitudinal steel. Meanwhile, for $M_i > M_{y(pre-jacket)}$, the yield point is obtained by the jacket tension steel because the existing tension steel has already yielded. The definition of the ultimate point is determined by comparing the ultimate tensile strain of the steel with the ultimate concrete compressive strain of the core, whichever is reached first, in this case obtained from the ultimate tensile strain of jacket steel.

Table 5 Comparison of cross-sectional discretization.

Section discretization	w/Initial load	Monolithic approach		
	Case-1	Case-2	Case-3	Case-4
Core	Confined-2	Confined-1	Confined-1	Confined-1
Existing outer cover	Confined-3	Unconfined	Confined-3	Confined-1
Inner jacket	Confined-3	Unconfined	Confined-3	Confined-1
Existing inner cover	Unconfined	Unconfined	Unconfined	Unconfined
Jacket cover	Unconfined	Unconfined	Unconfined	Unconfined

Notes:
a. $P = 0.13P_u$
b. Confined-1: confined by existing stirrups
c. Confined-2: confined by existing and jacket stirrups
d. Confined-3: confined by jacket stirrups

It can also be seen from Table 6 that the results of the M-φ relationship between case 1 and case 4 show an ultimate strength difference of ±7%. The monolithic approach of case 4 is not recommended, because it will overestimate the capacity of the section. The section capacity from the monolithic approach for case 2 and case 3 is broadly the same, which is due to the differences in the constitutive model used for discretization of the existing outer cover and the inner jacket, which have a stress difference of only ≤ 1%. Based on this, a recommendation that is safe and practical for engineering practice is to use the monolithic approach for case 2, where the jacket material is modeled as unconfined concrete.

Figure 9 shows the stress-strain profile at the ultimate curvature, in which the comparison of stress in the four cases shows slight differences. This proves the hypothesis that the strain profile of case 1 does not have strain compatibility.

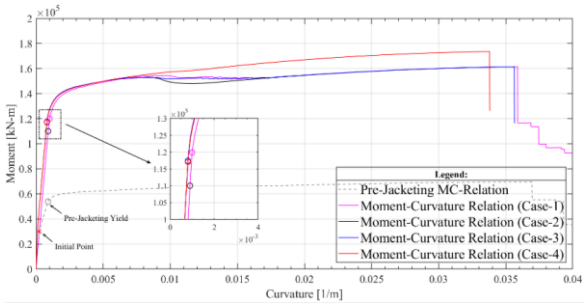

(a)

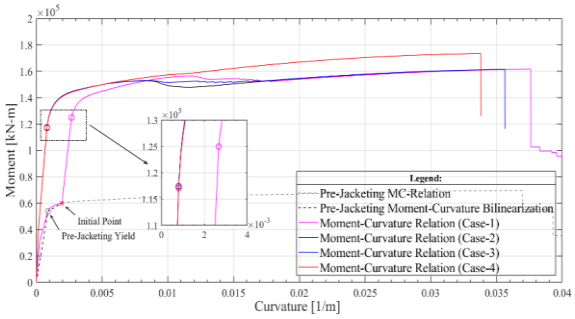

(b)

Figure 8 Comparison between M-φ relationship considering the initial load with a monolithic approach: (a) $M_i \leq M_{y(pre-jacket)}$, (b) $M_i > M_{y(pre-jacket)}$.

Table 6 Comparison of M-φ parameter result from monolithic approach.

Parameter	Case 1	Case 2	Case 3	Case 4
		$M_i \leq M_{y(pre-jacket)}$		
φ_y (1/m)	0.000998	0.000808	0.000808	0.000812
φ_u (1/m)	0.035870	0.035630	0.035630	0.033790
M_y (kN-m)	119890.32	117427.8484	117423.0510	117100.6825
M_u (kN-m)	161598.79	161455.9109	161511.7650	173556.4952
		$M_i > M_{y(pre-jacket)}$		
φ_y (1/m)	0.002676	0.000808	0.000808	0.000812
φ_u (1/m)	0.037577	0.035630	0.035630	0.033790
M_y (kN-m)	124966.46	117427.8484	117423.0510	117100.6825
M_u (kN-m)	161650.75	161455.9109	161511.7650	173556.4952

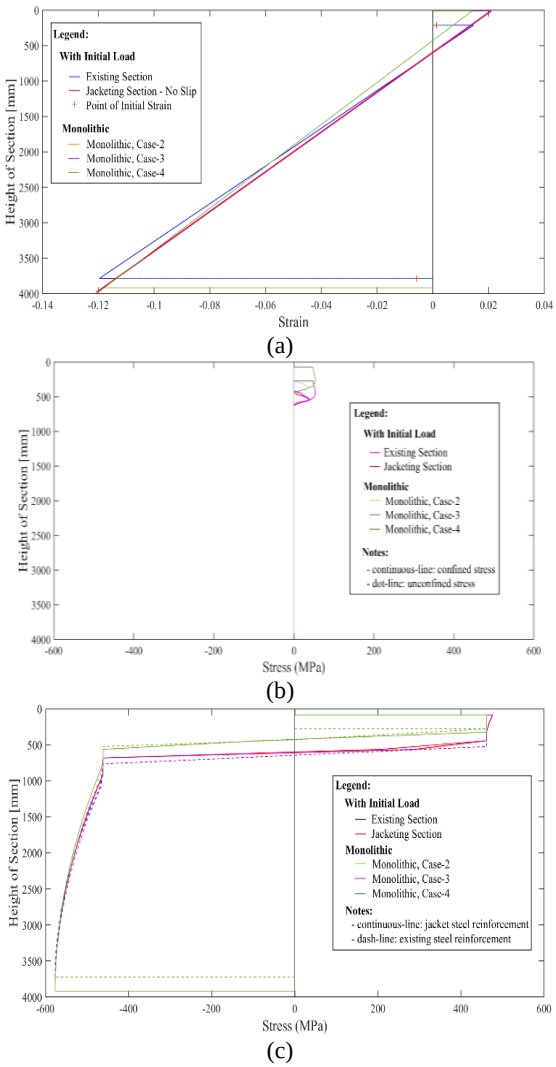

Figure 9 Stress-strain profile at ultimate curvature: (a) strain, (b) concrete stress, (c) steel stress.

3.2.4 Interface Slip Effect

Figure 10(a) shows that the section capacity drops when the interface slip is considered in the non-linear RC section analysis with jacketing. Basically, it shows that the stiffness as well as the section capacity will drop to become very close to the existing RC section values if the coefficient is close to zero (a very minimal bond). As can be seen from Figure 10(a), the neutral axis position for

each slip coefficient value (μ) changes when compared to the condition without slip (fully composite).

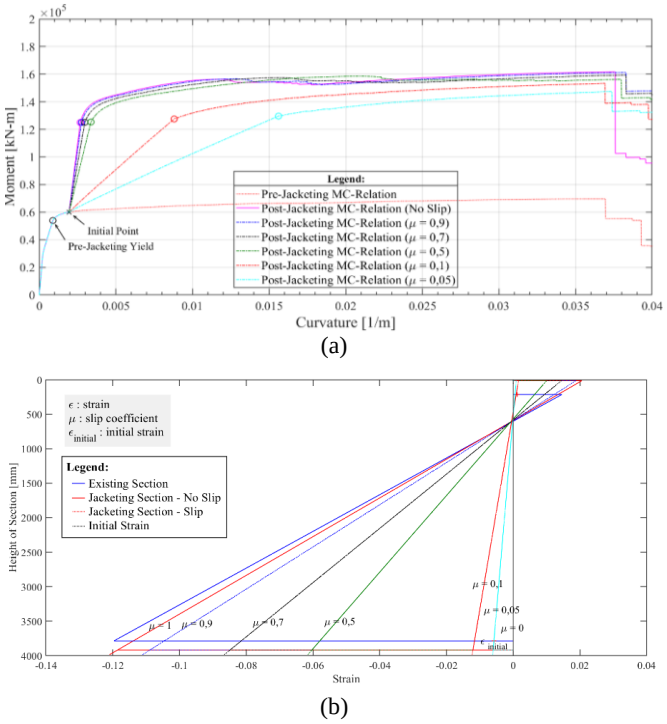

Figure 10 Cross-section section capacity with interface slip effect: (a) M-φ relationship, (b) strain profile at ultimate curvature.

Referring to Figure 10(a), it was also found that the section capacity decreases with a slip coefficient of 0.5-0.9, but it does not have a significant effect. It can be inferred that by only using one of the roughing methods on the interface surface area is sufficient and the use of shear connectors can be reduced, which is consistent with previous researches [2,5,7]. In the case of μ = 0, where jacket slip completely absent because the jacket encloses the existing pier, there must be some geometric compatibility between the jacket and the existing pier, since the jacket has to bend with the existing pier and is thus forced to follow the curvature of the existing section (at least partially).

4 Seismic Performance of RC Bridges

To get a better understanding of the seismic performance of retrofitted bridge piers with concrete jacketing considering the initial load and interface slip, pushover analysis was used to calculate the performance level of the bridge. The

seismic performance of RC bridge was conducted according to NCHRP Synthesis 440 [19].

Figure 11 illustrates the research methodology used in this study, where the seismic performance was analyzed for three cases, i.e. the performance of the existing bridge with and without displacement load, respectively, and the performance of the retrofitted bridge. A comparison between the three cases was made, where for the retrofitted bridge also the difference in seismic performance level was assessed using the monolithic approach as input for the modeling of the plastic hinge of retrofitted bridge piers. The capacity of the concrete components to resist all seismic demands except shear was assessed based on the expected material strength for unconfined and confined concrete as well as the reinforcing steel to provide a more realistic estimate of the earthquake load capacity [15,17,18].

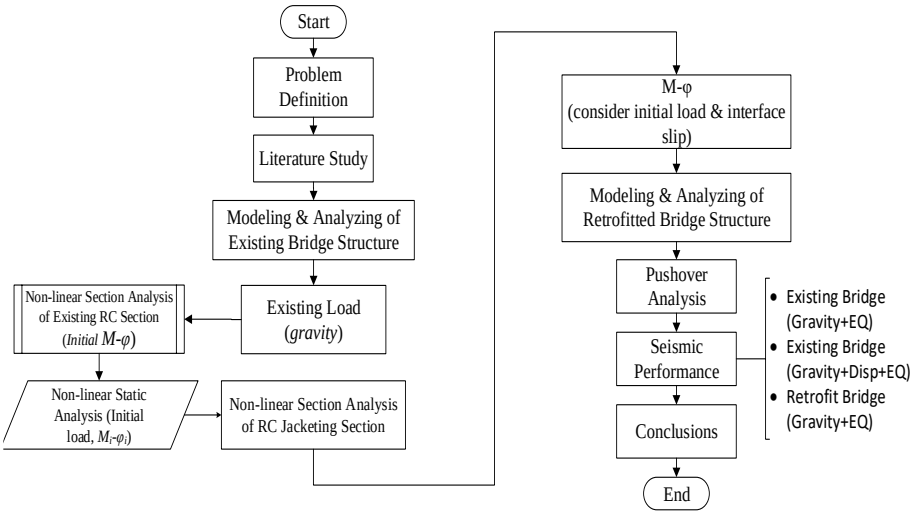

Figure 11 Research methodology.

4.1 Structural Modeling and Assumptions

This section discusses the general structural modeling and assumptions that were used in evaluating the seismic performance of the retrofitted bridge. As has already been mentioned in Section 2, the structural system of the bridge contains two types of spans. For simplification of the structural modeling, only the continuous-integral spans were modeled (P1-P2-P3-P4), because the bridge's response is determined by the continuous-integral spans.

The structural modeling and analysis of the bridge structure were carried out with the Midas Civil software by using beam elements to create the piers, PCI beams,

and bent caps. An elastic link element and a linear spring were used to model the bearings and piles respectively, and shell finite elements were used to model the slab. A rigid connection between the column bent top and the superstructure was idealized to model the continuous-integral spans, a pinned connection was specified at the pile base through joint restraints for all translation degrees of freedom, and a pinned boundary condition was defined at each end of the superstructure. The dynamic behavior of the structural system was calculated with the effective stiffness value according to FEMA-273 Table 6-4 [20] and the seismic load demand was based on the new Indonesian Bridge Seismic Design Code (SNI) [21], in which this bridge structure is classified as Other Bridges with site class SD and a PGA of 0.448 g.

4.2 Plastic Hinge Model

The inelastic properties of the bridge structure elements were modeled using the moment-rotation hinge backbone curve. It can be seen from Table 7 that the retrofitted RC bridge pier section was modeled as uncoupled hinge without axial-moment interaction to prevent the software (Midas Civil) from automatically interpolating the moment-rotation hinge backbone curve [12]. The plastic hinge model definition for all hinges was adopted from Aviram *et al.* [17]. The plastic hinge modeling of the bridge structure elements in Midas Civil software is illustrated in Figure 12.

Table 7 Inelastic property of bridge structure elements.

RC section	Non-Linear Hinge Options	
	Uncoupled hinge M3	Interaction PMM hinge
PCI beam	x	
Pierhead	x	
Existing RC bridge pier		x
Retrofitted RC bridge pier	x	

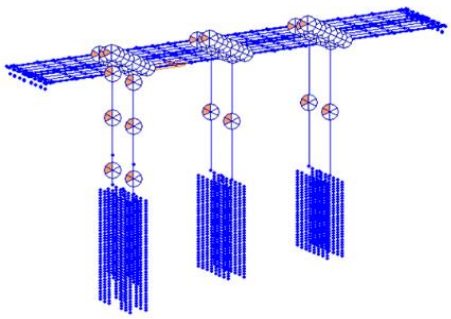

Figure 12 Plastic hinge model of the bridge structure elements.

4.2.1 Retrofitted Elements

The inelastic properties of the elements, retrofitted by concrete jacketing (pier P2 bottom) were calculated considering the initial load and interface slip parameters, based on Section 3. The contribution of the FRP jacket to the non-linear section analysis of the retrofitted section was not considered because the confining effect can be assumed as negligible for rectangular sections with dimensions exceeding 900 mm [22]. The initial load parameter was obtained by performing non-linear static analysis on the existing structure, using load control of gravity and pier displacement to obtain the initial moment value and use it to determine the condition of the existing bridge piers and also as the initial point for calculating the moment-curvature relationship of the RC section with jacketing [12]. It can be seen from Table 8, that bridge pier P2 has undergone plastic deformation as the longitudinal reinforcing steel has already exceeded the first yield point, while the other bridge piers (P3 and P4) are still in elastic condition.

Table 8 Existing bridge pier conditions due to displacement load.

Bridge Pier	Location	Condition	Explanation
P2	Bottom	$M_i > M_{y(pre-jacket)}$	Yield
	Top	$M_i > M_{y(pre-jacket)}$	Yield
P3	Bottom	$M_i < M_{y(pre-jacket)}$	Elastic
	Top	$M_i < M_{y(pre-jacket)}$	Elastic
P4	Bottom	$M_i < M_{y(pre-jacket)}$	Elastic
	Top	$M_i < M_{y(pre-jacket)}$	Elastic

Furthermore, the interface slip parameter was checked by comparing the nominal horizontal shear strength (V_{nh}) and the factored shear force (V_u) in the element. As can be seen in Table 9, by checking the calculations that were already performed, interface slip does not occur and the retrofit section is assumed to be fully composite. The results for the moment-curvature relationship of the retrofitted bridge pier elements by concrete jacketing are presented in Figure 13. It should be noted that due to limitations of the software that was used to determine the seismic performance of the bridge (i.e. the software cannot consider both birth and death time of the jacketing), the strategy used in the modeling of the plastic hinge of the retrofitted elements was normalized from the initial point of the moment-curvature of the RC section with jacketing. This was done because the existing bridge pier section P2 was already in plastic condition by the pushover initial load of gravity and displacement so that the Midas Civil software analyzed the pushover load with an assumption of residual value of the inelastic property of the RC section with jacketing, calculated from the initial point.

Table 9 Calculation check of interface slip parameter.

Parameters	Description	Unit	Direction		Ref
			Major	Minor	
b_v	width of the contact surface	mm	4000	3500	Retrofit Drawing
d	distance from extreme compression fiber to centroid of longitudinal tension reinforcement	mm	3918	3418	-
ϕ	strength reduction factor	-	0.75	0.75	ACI-318-14, 5.3.1
$d_{b,f}$	nominal diameter of shear friction bar	mm	13-300	13-300	Retrofit Drawing
n-$d_{b,f}$	number of shear friction bars	-	16	16	Retrofit Drawing
	Shear Connector Check				
A_{vf}	area of shear friction reinforcement	mm^2	213.72	213.72	-
fc'	concrete compressive strength	MPa	30	30	DED, SNI 2052:2017
#REF!	yield strength of reinforcing steel	MPa	420	420	DED, SNI 2052:2017
ρ_v	ratio of reinforcement area to area of contact surface	-	0.002023	0.002023	-
(a) $A_{vf,min}$		mm^2	848.97	848.97	ACI-318-14-1, 16.4.6.1
(b) $A_{vf,min}$	minimum area of shear transfer reinforcement	mm^2	875	875	ACI-318-14-1, 16.4.6.1
$A_{vf,min}$: greater of (a) & (b)		mm^2	875	875	ACI-318-14-1, 16.4.6.1
	Check: $A_{vf} > A_{vf,min}$		OK	OK	
	Interface Slip Check				
V_u	factor shear force at section	kN	725.79	1010.51	Midas Civil Output
$\phi 3{,}5 b_v d$	ACI-318-14 requirement to determine nominal interfce shear strength	kN	41139.00	31402.88	ACI-318-14, 16.4.4
Check: $Vu \leq \phi 3{,}5 b_v d$	if yes, Vnh shall be calculated in accordance with Table 16.4.4.2	-	Yes	Yes	ACI-318-14, Table 16.4.4.2
$V_{nh} = 0{,}55 b_v d$	nominal interface shear strength	kN	8619.6	6579.65	ACI-318-14, 16.4.4.2
	Cek, $\phi V_{nh} \geq V_u$:		OK-No Slip	OK-No Slip	ACI-318-14, 16.4.3.1

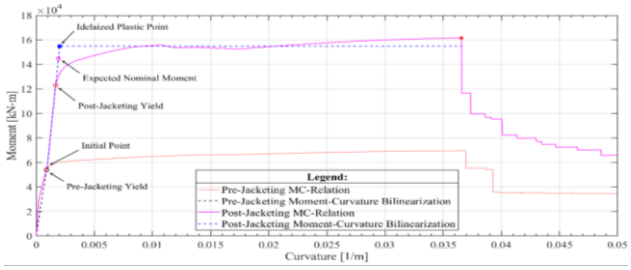

(a)

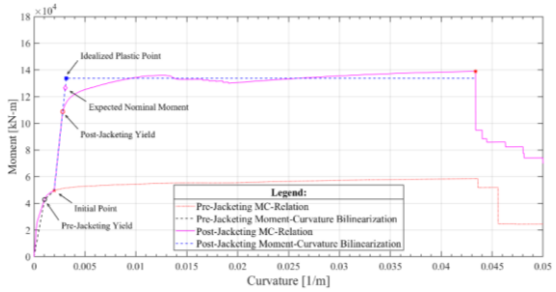

(b)

Figure 13 Moment-curvature of retrofitted bridge pier P2: (a) major axis, (b) minor axis.

Table 10 presents a summary of the bridge pier plastic hinge parameters, where CJ and SJ are defined as bridge piers retrofitted with concrete jacketing and steel jacketing, respectively, while Ex is defined as an existing bridge pier. When the contact surfaces of the old concrete are not roughened and interface slip is likely to occur in the retrofitted section, the slip coefficient can be assumed to be 0.9 [2].

Table 10 Summary of bridge pier plastic hinge parameters.

Pier	Section Direction	Axial Load (kN)		Generalized Load Deformation								
				Rotation (rad)					Moment (kN-m)			
		Location	Load	θyield_B	θ-ult	θp_C	θ_D	θ_E	M_B	M_C	M_D	M_E
P2	Major	CJ-base	18152	0.00219	0.07260	0.06849	0.08257	0.10370	89790	99913	19983	19983
		CJ-top	16939	0.00249	0.03455	0.03206	0.03847	0.04809	151378	147582	29516	29516
		CJ-base-case2	18152	0.00214	0.07260	0.07047	0.08456	0.10570	146847	152336	30467	30467
		CJ-top-case2	16939	0.00214	0.07260	0.07047	0.08456	0.10570	143377	150652	30130	30130
		CJ-base-case4	18152	0.00227	0.06885	0.06658	0.07989	0.09987	144789	160951	32190	32190
		CJ-top-case4	16939	0.00227	0.06885	0.06658	0.07990	0.09987	142855	159048	31810	31810
		SJ-base	13811	0.00211	0.05695	0.05484	0.06581	0.08226	207300	223400	44680	44680
		SJ-top	13302	0.00211	0.05736	0.05525	0.06630	0.08287	207000	223400	44680	44680
		Middle-Ex-base	16939	0.00197	0.03121	0.02924	0.03509	0.04386	59212	60370	12074	12074
		Middle-Ex-top	13811	0.00195	0.03262	0.03067	0.03681	0.04601	54331	55890	11178	11178
	Minor	CJ-base	18152	0.00242	0.08436	0.07791	0.09430	0.11888	77072	84270	16854	16854
		CJ-top	16939	0.00304	0.04367	0.04064	0.04877	0.06096	125951	128082	25616	25616
		CJ-base-case2	18152	0.00244	0.08477	0.08233	0.09880	0.12349	132584	131345	26269	26269
		CJ-top-case2	16939	0.00244	0.08477	0.08233	0.09879	0.12349	128350	137284	27457	27457
		CJ-base-case4	18152	0.00262	0.07894	0.07631	0.09158	0.11447	126638	140256	28051	28051
		CJ-top-case4	16939	0.00262	0.07894	0.07632	0.09158	0.11448	124934	138604	27721	27721
		SJ-base	13811	0.00242	0.06922	0.06680	0.08016	0.10020	182100	197600	39520	39520
		SJ-top	13302	0.00242	0.06985	0.06743	0.08092	0.10114	181900	197600	39520	39520
		Middle-Ex-base	16939	0.00241	0.03636	0.03394	0.04073	0.05092	50010	50906	10181	10181
		Middle-Ex-top	13811	0.00242	0.03841	0.03599	0.04319	0.05399	45867	47191	9438	9438
P3	Major	Base	16760	0.00209	0.07152	0.06943	0.08331	0.10414	58956	63607	12721	12721
		Top	11911	0.00206	0.07092	0.06885	0.08263	0.10328	52110	56196	11239	11239
	Minor	Base	16760	0.00256	0.08443	0.08187	0.09824	0.12280	49743	53526	10705	10705
		Top	11911	0.00256	0.08371	0.08115	0.09739	0.12173	43399	47282	9456	9456
P4	Major	Base	19087	0.00227	0.07723	0.07496	0.08995	0.11244	58995	62958	12592	12592
		Top	13825	0.00224	0.07658	0.74347	0.08922	0.11152	51099	54961	10992	10992

Table 11 Summary of PCI beam and pierhead plastic hinge parameters.

Element	θ_y	My	θ_u	M_u	$\theta_{y\text{-}eq}$	$M_{y\text{-}eq}$	L-beam
PCI-P2 Left	0.00288	20210	0.03509	25660	0.00346	24320	36.350
PCI-P2-P3-P4 Left	0.00235	18960	0.02943	26440	0.00321	25860	35.600
PCI-P4 Right	0.00240	21090	0.03085	29140	0.00335	29090	35.600
Pierhead	0.00141	62520	0.06495	106800	0.00222	98550	40.100

where, θ_y and θ_u are the yield and ultimate rotation in radians, respectively; M_y and M_u are the yield and ultimate moment in kN-m, respectively; $\theta_{y\text{-}eq}$ and $M_{y\text{-}eq}$ are the equivalent yield rotation in radians and the equivalent yield moment in kN-m, respectively; and L-beam is the length of the PCI beam in meters.

4.3 Performance Level of RC Bridge

Figure 14(a) shows the pushover analysis result in the longitudinal direction of the bridge. This curve shows the results for the retrofitted condition with the plastic hinge model that considers the initial load condition.

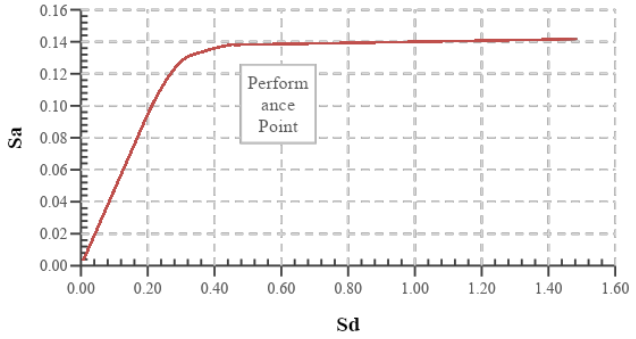

(a)

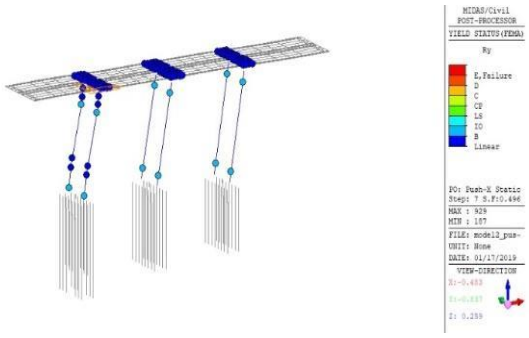

(b)

Figure 14 Pushover analysis results: (a) pushover capacity curve, (b) plastic hinges mechanism at performance point.

It was shown that the performance level of the retrofitted bridge structure was 'operational'. The node displacements and drift ratios are shown in Table 12. In the FEM model, as shown in Figure 14(b), each small circle denotes a plastic hinge model. Note that all members were assigned with two plastic hinge models at both ends, except for Pier P2. For Pier P2, plastic hinge models were inserted at both ends and at the section transition from original to jacketed section. In Figure 14(b), the plastic hinge models that remained elastic are indicated with blue color, while the plastic hinge models that reach plastic condition are indicated with cyan color.

Table 12 Performance level of retrofitted RC bridge.

Pushover direction	Node control displacement	Drift ratio (%)	Performance level	
			Structure	Element
Longitudinal	0.4675	1,0013	Operational	B - IO
Transversal	0.2467	0,5279	Fully operational	Elastic

A comparison of the seismic performance of the bridge before and after retrofitting was conducted by reviewing several cases. The longitudinal pushover capacity curve results are shown in Figure 15 and Table 13. The explanation of these cases is as follows:

1. TJ-1: Grav+EQ, un-retrofitted bridge structure with pushover initial loading only gravity;
2. TJ-2: Grav+Disp+EQ, un-retrofitted bridge structure with pushover initial loading of gravity and pier displacement;
3. J1-1: Grav+EQ, retrofitted bridge structure with pushover initial loading only gravity and plastic hinge model considering initial load;
4. J0-1: Grav+EQ, retrofitted bridge structure with pushover initial loading only gravity, plastic hinge model using a monolithic approach, and inner jacket and cover jacket modeled as unconfined material;
5. J0-2: Grav+EQ, retrofitted bridge structure with pushover initial loading only gravity, plastic hinge model using a monolithic approach, and inner jacket and cover jacket modeled as unconfined material.

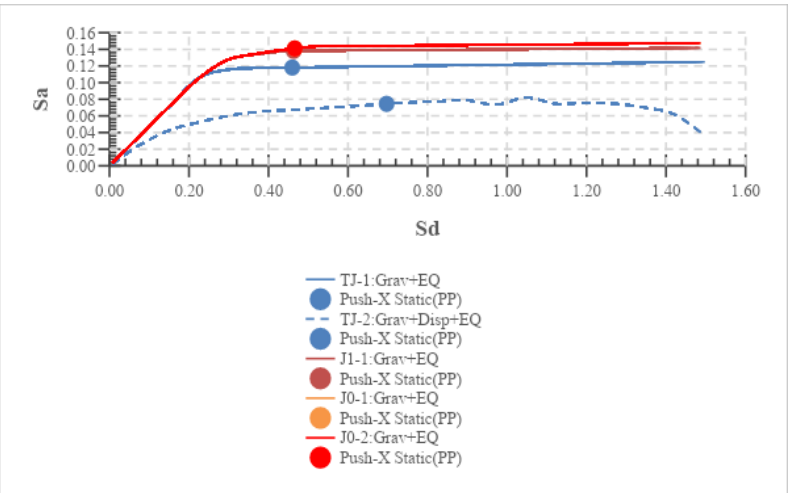

Note: The curves for models J1-1 and J0-1 coincide.

Figure 15 Comparison of pushover capacity curves.

From Figure 15 it is clear that the application of jacketing to the existing bridge structure can increase the capacity of the bridge by almost 15% (J1-1 to TJ-1) and around 46% (J1-1 to TJ-2), respectively.

It was also found that the pushover capacity curve of the plastic hinge model using initial load compared with the monolithic approach shows differences of only ±2.0%, not significantly affecting the bridge structure capacity. This is because the section capacity of the retrofitted section also shows only slight differences of ≤ 7%. Moreover, the bridge capacity response is not only determined by the retrofitted bridge pier P2 but also by the contribution of piers P3 and P4, which are still in elastic condition as the bridge structural system is continuous-integral type. To summarize, the seismic performance level of the bridge structure was the same, i.e. 'operational', using either the plastic hinge model of initial load or the monolithic approach.

Table 13 Comparison of performance level of RC bridge.

Pushover case	Node control displacement	Drift ratio (%)	Performance level (structure)
TJ-1:Grav+EQ	0.4606	0.99%	Fully operational
TJ-2:Grav+DISP+EQ	0.6983	1.49%	Operational
J1-1:Grav+EQ	0.4675	1.00%	Operational
J0-1:Grav+EQ	0.4702	1.01%	Operational
J0-2:Grav+EQ	0.4702	1.01%	Operational

5 Conclusions

The following conclusions can be drawn from the results of the investigation of the seismic performance of RC hollow rectangular bridge piers retrofitted with concrete jacketing considering initial load and interface slip:

1. The application of jacketing to the damaged bridge pier could increase the capacity of the bridge pier structure by almost 15% compared to the existing undamaged bridge pier structure and around 46% compared to the damaged bridge pier structure.
2. The results of the pushover analyses using a plastic hinge model based on a monolithic approach and considering initial load showed the same performance level, i.e. 'operational'. This can be expected considering that the maximum moment capacity only differs by less than 7%.
3. Interface slip with a slip coefficient of < 0.5 will significantly reduce the section capacity of the retrofitted section. It can also be concluded that roughing the interface surfaces area is adequate to provide sufficient interface shear strength, so the use of shear connectors can be reduced. From a practical engineering perspective, the interface slip in retrofitted bridge piers can be neglected or fully composite condition can be assumed because the nominal

shear strength at the interface of the new and the old concrete is adequate to prevent slip, provided that the surface of the old concrete has been well roughened before jacketing.

4. A conservative and practical recommendation for modeling the stress-strain relationship of the jacket material in engineering practice is to model it as unconfined concrete.

References

[1] Chen, W.F. & Duan, L., *Bridge Engineering in Indonesia*, Handbook of International Bridge Engineering, CRC Press Taylor & Francis Group, LLC, pp. 951-1016, 2014.

[2] Campione. G., Fossetti, M., Giacchino. C. & Minafò, G., *RC Columns Externally Strengthened with RC jackets*, Materials and Structures/ Matériaux ET Constructions, **47**(10), pp. 1715-1728, 2014.

[3] FIB Task Group 7.4, *FIB Bulletin No. 39: Seismic Bridge Design and Retrofit – Structural Solutions*, Lausanne, Switzerland: FIB (Fédération Internationale du Béton), 2007.

[4] Ersoy, U., Tankut, A.T. & Suleiman, R., *Behavior of Jacketed Columns*, ACI Structural Journal, **90**(3), pp. 288-293, 1993.

[5] Júlio, E.N.B.S., Branco, F.A.B. & Silva, V.D., *Reinforced Concrete Jacketing - Interface Influence on Monotonic Loading Response*, ACI Structural Journal, **102**(2), pp. 252-257, 2005.

[6] Júlio, E.N.B.S. & Branco, F.A.B., *Reinforced Concrete Jacketing – Interface Influence on Cyclic Loading Response*, ACI Structural Journal, **105**(4), pp. 1-7, 2008.

[7] Vandoros, K.G. & Dritsos, S.E., *Concrete Jacket Construction Detail Effectiveness when Strengthening RC Colum*ns, Construction and Building Materials, **22**(3), pp. 264-276, 2008.

[8] Alhadid, M.M.A. & Youssef, M.A., *Analysis of Reinforced Concrete Beams Strengthened Using Concrete Jackets*, Engineering Structures, **132**, pp. 172-187, 2017.

[9] The National Standardization Agency of Indonesia (BSN), SNI 03-1726-2002 *Seismic Provisions for Buildings Structures*, 2002. (Text in Indonesian)

[10] LAPI ITB, *Cisomang Bridge Structural Analysis Report*, PT. LAPI ITB, Bandung, 2017.

[11] Park, R. & Paulay, T., *Reinforced Concrete Structures*, John Wiley & Sons, Inc, 1975.

[12] Octora, D.D., *Analysis of Bridge Pier Retrofitted by Jacketing Method Considering the Initial Load and Interface Slip*, Master's Thesis, Institut Teknologi Bandung, Bandung, Indonesia, 2019.

[13] Ong, Y.C., Kog, Y.C., Yu, C.H. & Sreekanth, A.P., *Jacketing of Reinforced Concrete Columns Subjected to Axial Load*, Magazine of Concrete Research, **56**(2), pp. 89-98, 2004.
[14] Mander, J.B., Priestley, M.J.N. & Park, R., *Theoretical Stress-Strain Model for Confined Concrete*, ASCE Journal of Structural Engineering, **114**(8), pp. 1804-1826, 1988.
[15] Priestley, M.J.N., Seible, F. & Calvi, G.M., *Seismic Design and Retrofit of Bridges*, John Wiley & Sons, Inc., 1996.
[16] ACI Committee 318, ACI 318M-14 *Building Code Requirements for Structural Concrete*, American Concrete Institute, 2014.
[17] PEER, *Guidelines for Nonlinear Analysis of Bridge Structures in California*, Pacific Earthquake Engineering Research Center, 2008.
[18] Caltrans, *Seismic Design Criteria version 1.7*, California Department of Transportation, 2013.
[19] NCHRP, NCHRP Synthesis 440: *Performance-Based Seismic Bridge Design*, Washington, D.C.: Transportation Research Board, 2103.
[20] FEMA, FEMA-273: NEHRP Guidelines for The Seismic Rehabilitation of Buildings, Washington, D.C.: Federal Emergency Management Agency (FEMA), 1997.
[21] The National Standardization Agency of Indonesia (BSN), SNI 2833:2016: Design of Bridge Structures for Earthquake Loads, 2016. (Text in Indonesian).
[22] ACI Committee 440, ACI 440.2R-08: *Guide for the Design and Construction of Externally Bonded FRP Systems for Strengthening Concrete Structures*, American Concrete Institute, 2008.